Supplementary Information for:

Interaction with single-stranded DNA-binding protein localizes ribonuclease HI to DNA replication forks and facilitates R-loop removal

Table S1. *Escherichia coli* K-12 strains in this study

Strain	Relevant Genotype	Source
AB1157 and derivatives[a]		(Boyce & Howard-Flanders, 2003)
JC13509	sulB103 lacMS286 Φ80dIIIacBK1 argE3 his-4 thi-1 xyl-5 mtl-1 rpsL31 tsx	(Sandler et al., 2001)
SS9364	*rep::kan*	(Sandler, 2005)
SS9180	*rnhA::cat ilv-500::Tn10*	S. Sandler
SS10062	*ilv-500::Tn10*	S. Sandler
SS10032	*rnhA::cat del(proA)kan*	S. Sandler
SS6046	*recBCD::cat*	(Long, Massoni, & Sandler, 2010)
SS7329	*recB270(ts) recC271(ts) del(attB)::sulA-gfp*	S. Sandler
SS1651	*rnhA339::cat sulA-gfp*	(Sandler, 2005)
AL0454	*dnaA46(ts) tnaA300::Tn10*	(Hinds & Sandler, 2004)
SS10072	*rnhA::cat dnaA46(ts)*	S. Sandler
CP54	*rnhAK60E, cat*	P1 BW25113 with *rnhAK60E-cat* x JC13509 to Cm^r
CP58	*rnhAK60E, FLP scar*	CP54 with CAT removed
CP60	*rnhAK60E, cat ilv-500::Tn10*	P1.SS10062 x CP54 to Tc^r

CP62	*rnhAK60E, FLP scar proA::kan*	P1.SS10032 x CP58 to Kan^r
CP63	*rnhA$^+$, cat*	P1 BW25113 with *rnhA$^+$-cat* x JC13509 to Cm^r
CP64	*recG(kan ins)*	P1.EAW9 x JC13509 to Kan^r
CP65	*rnhA$^+$, FLP scar*	CP63 with CAT removed
CP70	*rnhA$^+$, cat ilv-500::Tn10*	P1.SS10062 x CP63 to Tc^r
CP71	*dnaA46(ts) tnaA300::Tn10 rnhA$^+$, cat*	P1. AL0454 x CP63 to Tc^r and Ts
CP79	*recG(kan ins) zic-4901::Tn10*	P1.CAG18492 x CP64
CP84	*rep::kan rnhA$^+$, FLP scar*	P1.SS9364 x CP65 to Kan^r
CP86	*rnhAK60E, FLP scar rep::kan*	P1. SS9364 x CP58 to Kan^r
CP88	*uvrD::kan*	P1. JDW1528 x CP65
CP89	*rnhAK60E, FLP scar uvrD::kan*	P1. JDW1528 x CP58 to Kan^r
CP90	*rnhAK60E, FLP scar recG::kan*	P1. EAW506 x CP58 to Kan^r
CP95	*uvrD::kan fadAB101::Tn10*	P1. CAG18496 x JDW1528 to Tc^r
CP96	*dinG::kan zbi-29::Tn10*	P1.CAG18493 x JW0784-

		1
CP119	*rnhAK60E, FLP scar rpoB2 rep::kan btuB::Tn10*	P1 JDW761 x CP86 to Rif^r
CP124	*rnhAK60E, FLP scar rep::kan rpoB8 btuB::Tn10*	P1. JDW756 x CP86
CP126	*rnhAK60E, FLP scar rep::kan pEAW903*	CP86 + pEAW903
CP127	*rnhA$^+$, FLP scar pEAW903*	CP65 + pEAW903
CP128	*rnhAK60E, FLP scar pEAW903*	CP58+ pEAW903
CP129	*rep::kan pEAW903*	CP84 + pEAW903
CP130	*rnhA$^+$, FLP scar rpoB8 (Q513P) btuB::Tn10*	P1. JDW756 x CP65
CP131	*rnhA$^+$, FLP scar rpoB2 (H526Y) btuB::Tn10*	P1. JDW761 x CP65
CP140	*rep::kan rpoB8 (Q513P) btuB::Tn10*	P1. JDW756 x CP84
CP141	*rep::kan rpoB2 (H526Y) btuB::Tn10*	P1. JDW761 x CP84
CP142	*rnhAK60E, FLP scar rpoB2 (H526Y) btuB::Tn10*	P1. JDW761 x CP58
CP143	*rnhAK60E, FLP scar rpoB8 (Q513P) btuB::Tn10*	P1. JDW756 x CP58
CP154	*rnhA::cat*	P1.SS10032 x JC13509 to Cm^r
CP165	*rnhA::cat zae502::Tn10*	P1.CAG18436 x CP154 to Tc^r
CP176	*rnhA$^+$, FLP scar polA12(ts)*	P1. CP63 x MM386
CP178	*rnhAK60E, FLP scar polA12(ts)*	P1. CP54 x MM386
CP179	*rnhA::cat polA12(ts)*	P1. SS1651 x MM386
CP206	*rnhAK60E, FLP scar recBCD::cat*	P1. SS6046 x CP58
RRL327	*rnhA-ypet-kan*	This study

RRL355	*Kan-mcherry-dnaN*	This study
RRL388	*frt-mcherry-dnaN*	This study
VV05	*dnaQ-mNeonGreen-kan*	This study
VV08	*rnhAK60E-ypet-kan*	This study
VV11	*frt-mcherry-dnaN rnhA-ypet-kan*	P1. RRL388 x RRL327
VV14	*rnhA-mNeonGreen-kan*	This study
Other strains used as P1 donors		
CAG18436	*uvrD::kan*	(MG1655 deriv.)
CAG18492	*zic-4901::Tn10*	(MG1655 deriv.)
EAW9	*recG(del)::kan*	(MG1655 deriv.)
CAG18496	*fadAB101::Tn10*	(MG1655 deriv.)
CAG18493	zbi-29::Tn10	(MG1655 deriv.)
JDW756	*rpoB8 (Q513P) btuB::Tn10*	(MG1655 deriv.)
JDW761	*rpoB2 (H526Y) btuB::Tn10*	(MG1655 deriv.)
JDW1528	*uvrD::kan*	(MG1655 deriv.)
EAW506	*recG::kan*	(MG1655 deriv.)
Other derivatives		
MM386	*lacZ53(Am), lambda-, relA1, rpsL151 (strR), polA12(ts), rha-5, deoC2*	W3110 derivative (Monk & Kinross, 1972)

[a]Only the relevant genotype is shown

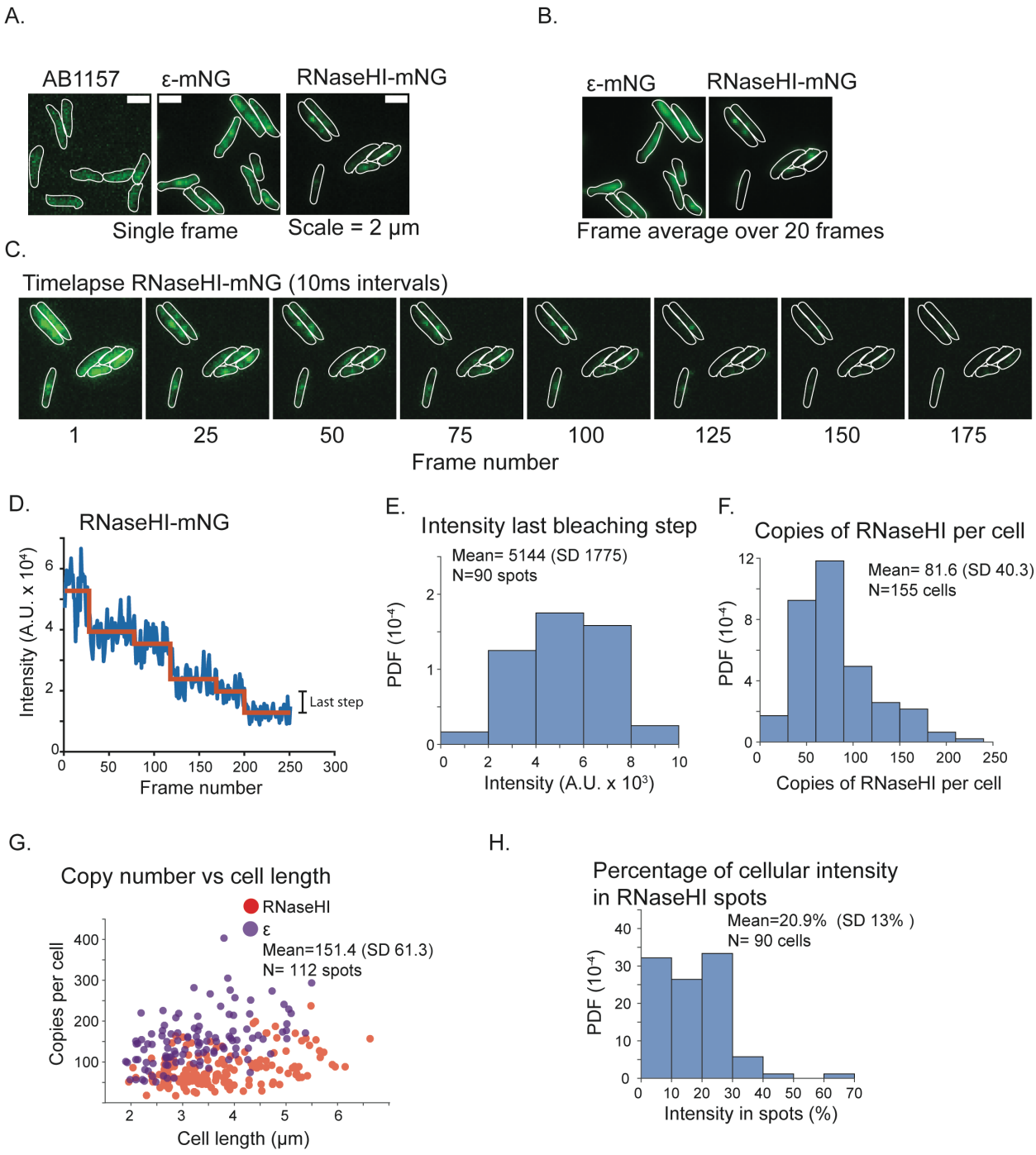

Figure S1. Estimation of copy number per cell and proportion DNA-bound molecules. (A) Representative pictures of AB1157, used as a control to estimate background endogenous fluorescence, and of cells carrying ε (the proofreading exonuclease subunit of DNA Pol III) and RNase HI fused to mNeonGreen. Camera integration time was of 10 milliseconds. **(B)** Frame

average of 20 pictures. **(C)** Example images of cells followed over 175 frames showing bleaching of fluorescence over time. **(D)** Example of the time-intensity profile of a single spot of RNase HI where a stepwise decrease of fluorescence can be observed. We used the difference in intensity in the last step as a measure of the intensity produced by a single molecule in our system. Note that the initial intensity, and the observation of multiple steps in the trace, are indicative of multiple copies of RNase HI being present in this spot. **(E)** Distribution of the intenstities of the last bleaching step for a population of spots. **(F)** Estimation of the copy number of RNase HI per cell obtained by dividing the integrated intensity of individual cells by our estimated intensity of a single molecule. **(G)** The relation between the estimated copy number and cell length is shown for RNase HI and for the DNA Pol III subunit ε. As expected, the copy number increases with cell length. Also, our estimate supports a higher copy number for ε compared to RNase HI, although this estimate is lower than a previously reported estimate of 270 copies (SD 160) (Reyes-Lamothe et al., 2010).**(E)** Estimation of the fraction of RNase HI copies that is bound to DNA obtained by dividing the summed intensity found in spots by the total intensity for individual cells.

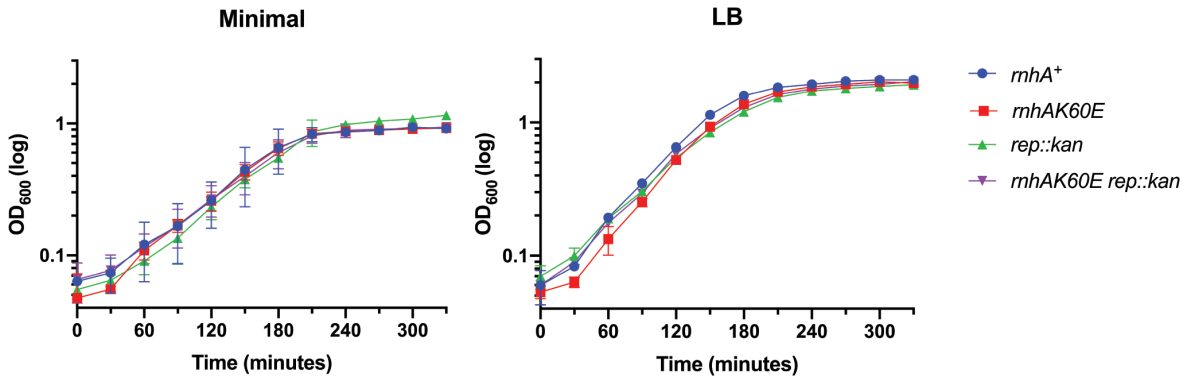

Figure S2. Growth curves of wild-type, *rnhA* and *rep E. coli* mutants. The OD_{600} time points of cultures grown in minimal (left) or LB (right) media shaking at 37°C. The growth curves were performed in triplicate for each strain and inoculated from different overnight cultures. The points represent the mean optical density at each time point and the error bars depict the standard deviation.

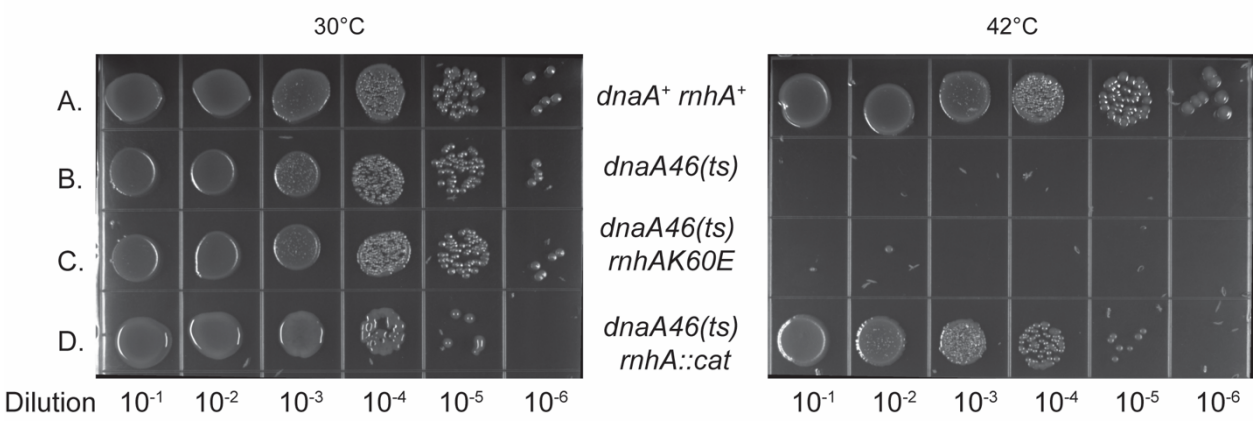

Figure S3. Complex formation with SSB is not required for suppresion of cSDR by RNase HI. Dilutions of overnight cultures grown in minimal medium (56/2) and plated on minimal medium. Plates were incubated at 30°C (left) or 42°C (right) for 36 hours or 24 hours, respectively. The images are the representative of a plating experiment performed in triplicate.

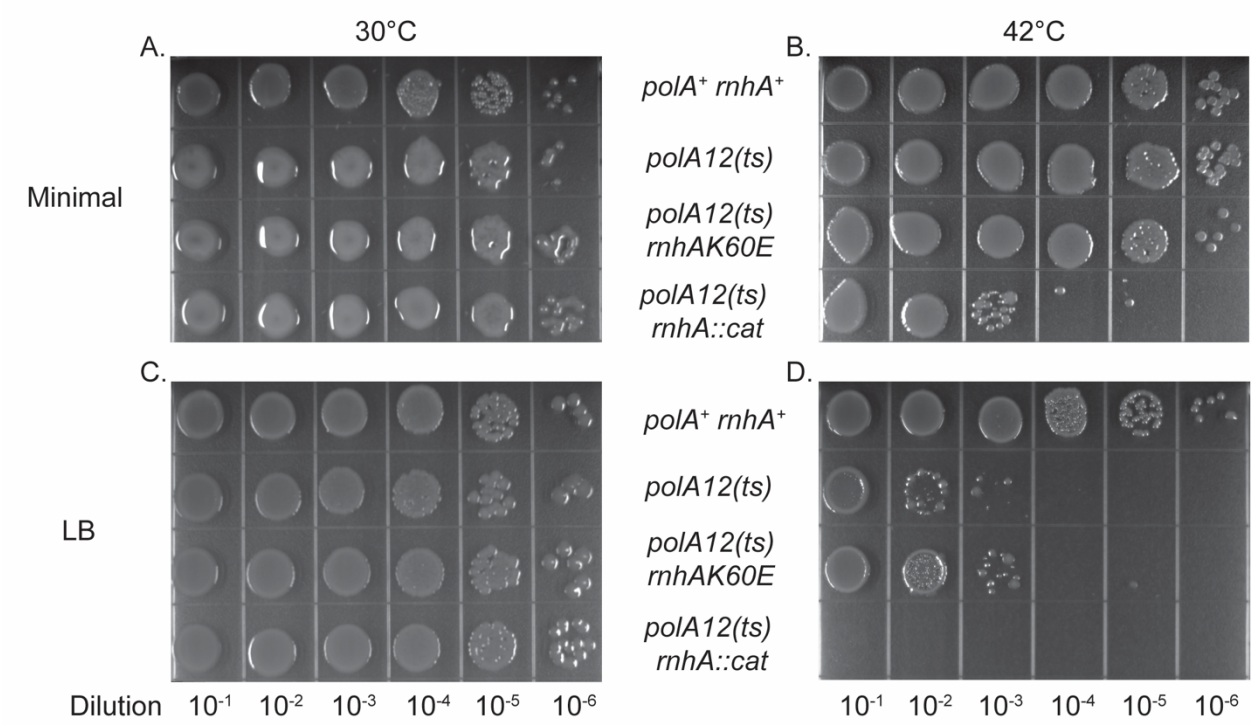

Figure S4. The loss of RNase HI localization does not affect RNase HI activity in DNA polymerase I-dependent pathways. Dilutions of overnight cultures grown in minimal medium (56/2) and plated on minimal medium (top, A and B) or LB (bottom, C and D). The plates were incubated at 30°C (left, A and C) or 42°C (right, B and D) for 36 hours or 24 hours, respectively. The images are the representative of a plating experiment performed in triplicate.

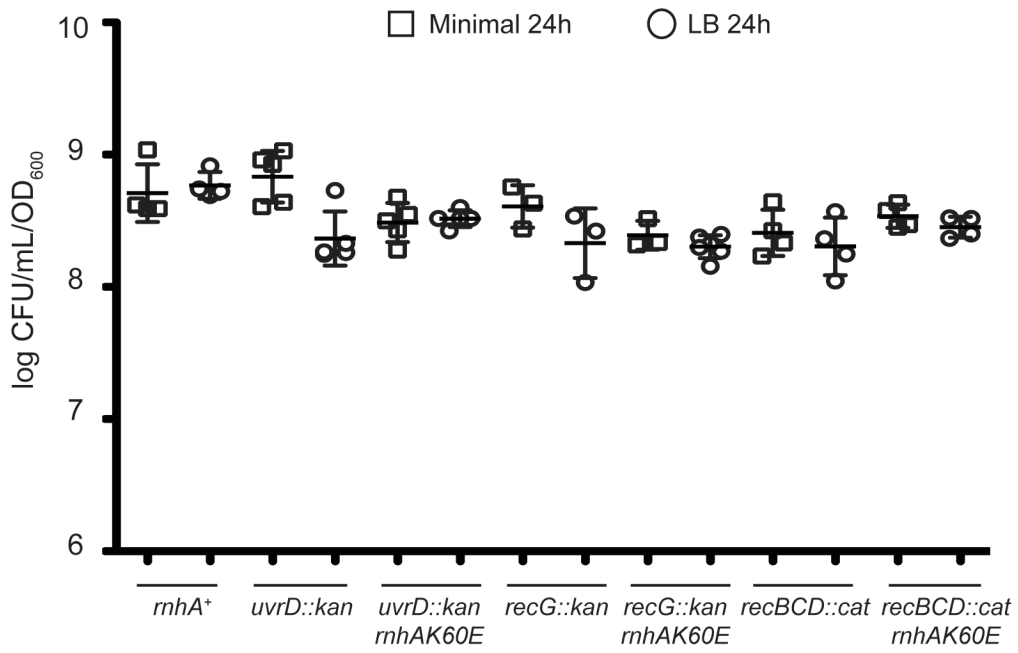

Figure S5. Plating efficiency of *uvrD*, *recG*, or *recBCD* mutants with or without *rnhAK60E* on minimal or rich media. The CFU/mL of each strain (normalized to OD_{600}) is plotted from overnight cultures diluted and plated on minimal (squares) or LB (circles) media. Colonies were quantitated after growth at 37°C for 24hrs. Each symbol is a single culture and the mean CFU/mL for each strain is represented by a black line. Error bars indicate the standard deviation.

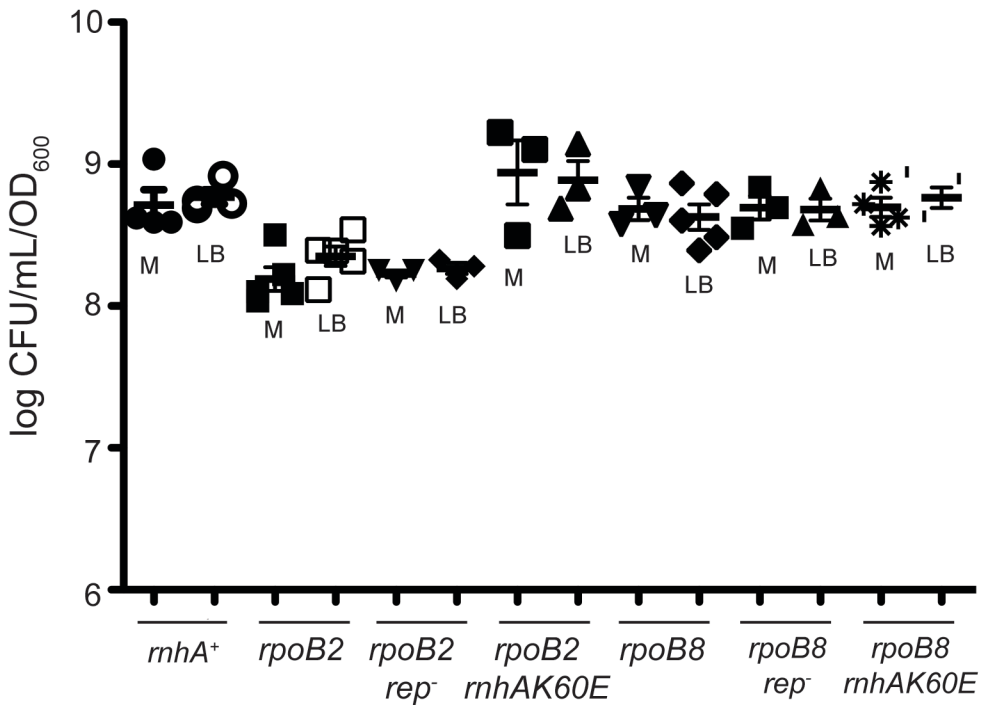

Figure S6. Plating efficiency of *rpoB* mutants with or without *rnhAK60E* or *rep::kan* on minimal or rich media. The CFU/mL of each strain (normalized to OD_{600}) is plotted from overnight cultures diluted and plated on minimal (M) or LB media. Plates were incubated at 37°C for 24 hours unless otherwise noted. Each symbol is a single culture and the mean CFU/mL for each strain is represented by a black line. The error bars indicate the standard deviation.

Supplementary References:

Boyce, R. P., & Howard-Flanders, P. (2003). Release of ultraviolet light-induced thymine dimers from DNA in E. coli K-12. 1964. *DNA Repair*, *2*(1927), 1280–1287.

Hinds, T., & Sandler, S. J. (2004). Allele specific synthetic lethality between priC and dnaAts alleles at the permissive temperature of 30°C in E. coli K-12. *BMC Microbiology*, *4*.

Long, J. E., Massoni, S. C., & Sandler, S. J. (2010). RecA4142 causes SOS constitutive expression by loading onto reversed replication forks in Escherichia coli K-12. *Journal of Bacteriology*, *192*(10), 2575–2582.

Monk, M., & Kinross, J. (1972). Conditional lethality of recA and recB derivatives of a strain of Escherichia coli K-12 with a temperature-sensitive deoxyribonucleic acid polymerase I. *J. Bacteriol.*, *109234*, 971–978.

Reyes-Lamothe, R., Sherratt, D. J., & Leake, M. C. (2010). Stoichiometry and architecture of active DNA replication machinery in Escherichia coli. *Science*, *328*(5977), 498–501.

Sandler, Steven J., McCool, J. D., Do, T. T., & Johansen, R. U. (2001). PriA mutations that affect PriA-PriC function during replication restart. *Molecular Microbiology*, *41*(3), 697–704.

Sandler, S J. (2005). Requirements for replication restart proteins during constitutive stable DNA replication in Escherichia coli K-12. *Genetics*, *169*(4), 1799–1806.